International Journal of Thermofluid Science and Technology (2021)
Volume 8, Issue 3, Paper No. 080304
https://doi.org/10.36963/IJTST.2021080304
Research Article

Magnetic Mixed Convection in a Vented Cavity with Volumetric Heat Generation or Absorption in Presence of a Cylindrical Obstacle

Md. Rubel Kazi, Mohammad Mokaddes Ali, Mijanul Hakim, Mizanur Rahman

Department of Mathematics, Mawlana Bhashani Science and Technology University, Tangail-1902, Bangladesh

ATICLE INFO

Received: 22 March 2021;
Received in revised form:
09 August 2021;
Accepted: 24 August 2021;
Published online:
03 September 2021

Keywords:
Magnetic field
Mixed convection
Heat generation or absorption
Vented square cavity
Finite element method

ABSTRACT

Effect of magnetic field on mixed convection in a vented square cavity with volumetric heat generation or absorption in presence of a cylindrical obstacle is analyzed numerically. The right vertical wall is considered at the hot temperature T_h and other partitions of the enclosure are adiabatic. The governing equations are solved based on finite element method. The relevant parameters in the current investigation, Prandtl number ($0.03 \leq Pr \leq 2.97$), Reynolds number ($100 \leq Re \leq 500$), Hartmann number ($0 \leq Ha \leq 30$), and volumetric heat generation or absorption parameter ($-10 \leq Q \leq 10$) are taken to find streamlines and heat transfer nature. Flow and temperature fields inside the enclosure are investigated for the mentioned parameters whereas effective trend is determined. On the other hand, heat generation or absorption parameter is found almost invariant for the streamline and isotherm plots. In addition, average Nusselt numbers are found to explain the heat transport inside the cavity and the average temperature are assumed to be a powerful tool to analyze and discussion.

1. Introduction

In the present, numerous scientists have given additional effort on mixed convection in different geometries because of its enormous applications in science and engineering fields as such heat exchangers, electronic cooling, solidification, food processing, float glass production, chemical processing equipment, nuclear reactors and solar collectors, etc. In addition, magnetic field effect on mixed convection flow and heat transfer have received considerable attentions due to it significant applications in crystal growth in liquids, electronic and micro-electronic devices, solar technologies and nuclear reactors, etc. Moreover, a few specialists have investigated mixed convection inside the enclosure with volumetric heat generation or absorption by numerically under thinking about its significance. Some existing literature review is listed from them.

Basak et al. [1] numerically studied the effects of different temperature conditions on mixed convection in lid driven cavity and observed that heat transfer rate reached to 1for the case of linearly heated wall and increased for cold right wall. They also found heat transfer rate strongly depend on Grashof and

*Corresponding e-mail: mrkazi318@gmail.com (Md. Rubel Kazi)

Nomenclature

d Dimension cylinder length (m)
D Non dimensional cylinder length
g Gravitational acceleration (ms^{-2})
k Thermal conductivity ($Wm^{-1}k^{-1}$)
L length of the cavity (m)
Nu Nusselt number
p Dimensional pressure (Nm^{-2})
P Dimensionless pressure
Pr Prandtl number
Re Reynolds number
Ri Richardson number
Ha Hartmann number
T Dimensional temperature (K)
u, v Dimensional velocity components (ms^{-1})
U, V Dimensionless velocity components
$\bar{V}$ Cavity volume (m^3)
w Height of the opening (m)
n non -dimensional distances either X or Y direction acting normal to the surface
x, y Cartesian coordinates (m)
X, Y Dimensionless Cartesian coordinates
$Q_\circ$ Heat generation or absorption coefficient
Q Dimensionless heat generation or absorption parameter
c_p Specific heat capacity ($Jkg^{-1}\ K^{-1}$)
$B_\circ$ magnetic induction (Wbm^{-2})
$\overline{V}$ cavity volume (m^3)

Greek Symbols

α Thermal diffusivity (m^2s^{-1})
β Thermal expansion coefficient (k^{-1})
ρ Density of the fluid (kgm^{-3})
θ Non dimensional temperature
υ Kinematic viscosity of the fluid (m^2s^{-1})
σ fluid electrical conductivity
μ Dynamic viscosity of the fluid

Subscripts

av Average
h Heated wall
i inlet state

Prandtl numbers. Later on, Basak et al. [2] performed a similar study for porous medium and found that Nusselt number increases from left edge to right edge of the bottom wall due to linearly heated left wall and cold right wall at the case of Re = 10 and 100 which was found irrespective for Prandtl and Darcy numbers. Hassan and Jamal [3] used finite volume method to investigate mixed convection in partially heated lid driven cavity with constant heat flux. They showed that temperature contours are nonlinear and peak shifts toward the center at greater Richardson number. It was also observed that the peak velocity near the right half of the cavity for top moving wall in that direction. Charttopadhyay et al. [4] conducted a parametric study for mixed convection in a lid driven porous cavity with sinusoidally heated wall and found heat transfer rate enhances with the increase in value of amplitude. Merkroussi et al. [5] studied mixed convection inside non-uniformly heated wavy cavity with top moving wall and showed that heat transfer rate strongly influenced due to the variable temperature at the wavy walls. Azizul et al. [6] analyzed numerically the heatline visualization of mixed convection in lid driven cavity with wavy bottom. Their results indicated that optimum heat transfer found for low Richardson number with one oscillation of wavy surface. Uddin et al. [7] used non-homogenous dynamic model to analyze the local and average Nusselt number for tubes with plain and uneven side walls. They found that higher heat transfer occurs at lower thermal Rayleigh number for the tube of having uneven vertical-walls whereas heat transfer rate become higher with the higher values thermal Rayleigh number for the tube of having smooth vertical-walls. The problem of natural convection flow and heat transfer in a wavy cavity was numerically investigated by Fayz-Al-Asad et al. [8]. In their study, a horizontal fin was attached to its hot vertical wall, and they observed the flow structure and temperature field affected with the length and location of the fin and mean Nusselt number increases with increasing Rayleigh number and fin length. Later on, Islam et al. [9] examine natural convection flow and heat transfer in a right-angle triangular cavity. They used finite element

method to simulate the problem considered. They noted that heat transfer rate reduces with increasing Hartmann number but increases for increasing buoyancy driven Rayleigh number. Rahman et al. [10] studied numerically heat-conducting cylinder effect on mixed convection inside the enclosure. They found that the heat transfer and flow structure characteristics strongly depend on the mixed convection and cavity aspect ratio. Later on, Rahman and Alim [11] carried out similar study by incorporating magnetic field and Joule heating effects. that noticed that streamlines and isotherms are strongly influenced due to variation in Ha, Re and Ri but little for Joule heating parameter. Ali et al. [12] used similar method to analyze magnetic field effect on mixed convection in a hexagonal cavity. They found that isotherms are remarkably modified for greater *Ri* and flow disseminations are additionally modified for each greater *Ri* and *Ha*. Oğlakkaya and Bozkaya [13] used DRBE method to investigate unsteady mixed convection in sinusoidal wavy lid driven cavity under the effect of magnetic field and concluded that flow and heat transfer rate augments for increasing *Ra* ($Ra \geq 10^4$) and decreases for higher *Ha* when undulation number kept fixed. Bakar et al. [14] analyzed magnetic inclination angle effect on flow and heat transfer in a 2D cavity with top moving wall and the flow field was retarded due to magnetic field effect whereas heat transfer rate increases for magnetic field angle. The problem of mixed convection flow in lid driven rectangular cavity with wavy top wall and rectangular heater was numerical studied by Sarkar et al. [15] and found that stronger magnetic field at higher Rayleigh number decreases the mixed convection heat transfer. Geridonmez and Oztop [16] used pseudo spectral method to investigate mixed convection in lid driven 2D cavity under the effect of partial magnetic field and found that convective heat transfer reduces for increase in length of the partial magnetic field. Chamkha [17] studied numerically combined convection in lid-driven cavity subjected to magnetic field effect for heat generation or absorption. They determined that velocity and heat transfer profile firmly rely upon the appearance of the magnetic field and Nu_{av} is lessened for assisting and opposing flow. Saha et al. [18] conducted a numerical study of mixed convection in lid driven cavity with uniformly heated bottom wall and taken into account internal heat generation or abortion effects and showed significant reduction in heat transfer rate for increased magnetic field strength. The flow and heat transfer distributions in mixed convection in a nanofluid filled lid driven enclosure considering heat generation or absorption were analyzed by Hussian et al. [19]. They performed that larger heat absorption provided greater heat transfer and opposite behavior is occurred for Hartmann number. In the forced convection region, heat generation or absorption inconsequential influenced but another is extensively affected.

Considering the literature survey presented in this paper, it is apparent that magnetic field effect on mixed convection in different geometries is of great interest to the researchers. Though researchers accomplished many studies of mixed and natural convection in different geometries presented in literature, heat generation / absorption effect on mixed convection heat transfer in a vented enclosure is rarely investigated. In the present study, the authors have studied mixed convection in a vented square cavity with a circular obstacle considering heat generation or absorption under the effect of magnetic field. To the best of the authors' knowledge, no work has been done yet relating to this issue. The main objective of this work is to numerically analyze the efficiency of dimensionless parameters such as Reynolds number, Hartmann and Prandtl numbers and heat generation or absorption parameter on mixed convection flow and heat transfer in a vented square cavity in order to control the fluid flow and heat transfer characteristics. As the present study offers a variety of improved performances in controlling flow and heat transfer mechanisms, the present investigation would be a great influence in the industrial and engineering appellations.

2. Physical model

The geometry consists of a square enclosure with length L is displayed in Fig. 1, and contains an adiabatic cylindrical obstacle with a diameter d placed at the center. The left lower corner considered as the origin in Cartesian coordinate system. A uniform constant temperature T_h is applied to the right vertical wall whereas remaining sidewalls are adiabatic. The inflow and outflow are set to the lower left and right top corner respectively and its width is w (w = 0.1L). Cold air is considered as working fluid that enters into the incoming path with uniform velocity u_i, and temperature T_i. The outflow of the working fluid has zero diffusion flux is considered for all pertinent variables. The non- slip boundary conditions is used for cylinder surface and side walls of the enclosure.

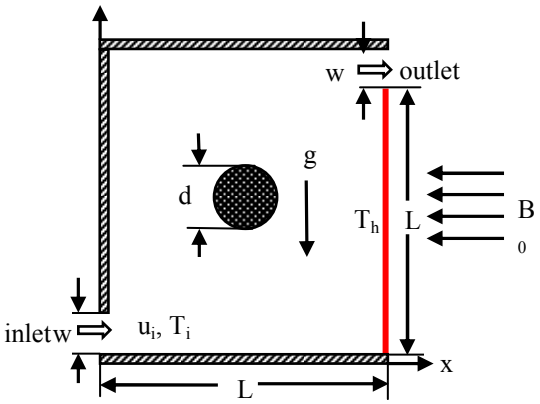

Fig. 1: Geometry of the physical

3. Mathematical modeling

The functioning flow is assumed to be steady, laminar, two-dimensional, and also considered as constant for every single fluid property. Under the Boussinesq approximation, the current problem can be described by using the dimensionless governing equations are as follows:

Continuity Equation

$$\frac{\partial U}{\partial X}+\frac{\partial V}{\partial Y}=0 \qquad (1)$$

Momentum Equations

$$U\frac{\partial U}{\partial X}+V\frac{\partial U}{\partial Y}=-\frac{\partial P}{\partial X}+\frac{1}{\mathrm{Re}}\left(\frac{\partial^2 U}{\partial X^2}+\frac{\partial^2 U}{\partial Y^2}\right) \qquad (2)$$

$$U\frac{\partial V}{\partial X}+V\frac{\partial V}{\partial Y}=-\frac{\partial P}{\partial Y}+\frac{1}{\mathrm{Re}}\left(\frac{\partial^2 V}{\partial X^2}+\frac{\partial^2 V}{\partial Y^2}\right)+Ri\theta-\frac{Ha^2}{\mathrm{Re}}V \qquad (3)$$

Energy Equation

$$U\frac{\partial \theta}{\partial X}+V\frac{\partial \theta}{\partial Y}=\frac{1}{\mathrm{Re}\,\mathrm{Pr}}\left(\frac{\partial^2 \theta}{\partial X^2}+\frac{\partial^2 \theta}{\partial Y^2}\right)+\frac{1}{\mathrm{Re}\,\mathrm{Pr}}Q\theta \qquad (4)$$

The dimensionless variables and parameters are characterized as:

$$X=\frac{x}{L},\ Y=\frac{y}{L},\ U=\frac{u}{u_i},\ V=\frac{v}{u_i},\ P=\frac{p}{\rho u_i^2},$$

$$D=\frac{d}{L},\ \theta=\frac{T-T_i}{T_h-T_i} \qquad (5)$$

$$\mathrm{Re}=\frac{u_i L}{\nu},\ \mathrm{Pr}=\frac{\nu}{\alpha},\ Ha=\sqrt{\frac{\sigma B_0^2 L^2}{\mu}},\ Q=\frac{Q_0 L^2}{\rho c_p}$$

$$Gr=\frac{g\beta(T-T_i)}{\nu^2}\ \text{and}\ Ri=\frac{Gr}{\mathrm{Re}^2} \qquad (6)$$

Equations (Eqs.1-4) are solved based on the following dimensionless boundary conditions:

At the inlet: $U=1,\ V=0,\ \theta=0$ (7a)

At the outlet: $P=0$ (7b)

At the cylindrical obstacle: $U=0, V=0,$

$$\frac{\partial \theta}{\partial n}=0 \qquad (7c)$$

At the heated wall: $\theta=1$ (7d)

At the adiabatic walls: $\left.\frac{\partial \theta}{\partial X}\right|_{X=0}=\left.\frac{\partial \theta}{\partial X}\right|_{Y=0,1}=0$ (7e)

The average Nusselt number at the heated wall and average temperature are defined as [10-12]:

$$Nu_{av}=\frac{1}{L_h}\int_0^{L_h}\frac{\partial \theta}{\partial X}dY \qquad (8a)$$

$$\theta_{av}=\int\frac{1}{V}\theta d\bar{V} \qquad (8b)$$

3.1. Computational Procedure

The governing equations (Eqs.1-4) along with boundary conditions (Eqs.7a-e) are solved by using Galerkin weighted residual finite element method which is well described by Taylor and Hood [20] and Dechaumphai [21]. The detail application of this method is

available in Refs. [22, 23].

3.2. Code Validation

The current work is extensively validated comparing with numerical results available in Rahman and Alim [11] and Bakar et al. [14]. The results are found in respect of average Nusselt number with considering similar cavity and boundary conditions of Rahman [11] is demonstrated in Table 1 which is contained a precise agreement. In addition, we have used our present code to simulate the problem mixed convection in a lid driven cavity in presence of inclined magnetic field [14] and plotted the obtained numerical results in Fig. 2 using streamlines and isotherms which shows a good agreement between our results and the results presented by Bakar et al. [14].

Table 1: Comparison of the average Nusselt number (Nu_{av})

Ha	Rahman and Alim [11] (Nu_{av})	Present study	Error (%)	Present study (Nu_{av})
0	2.20	2.22	0.90	4.60
10	2.11	2.15	1.89	4.38
20	1.82	1.88	3.29	4.00
50	1.18	1.27	7.62	3.45

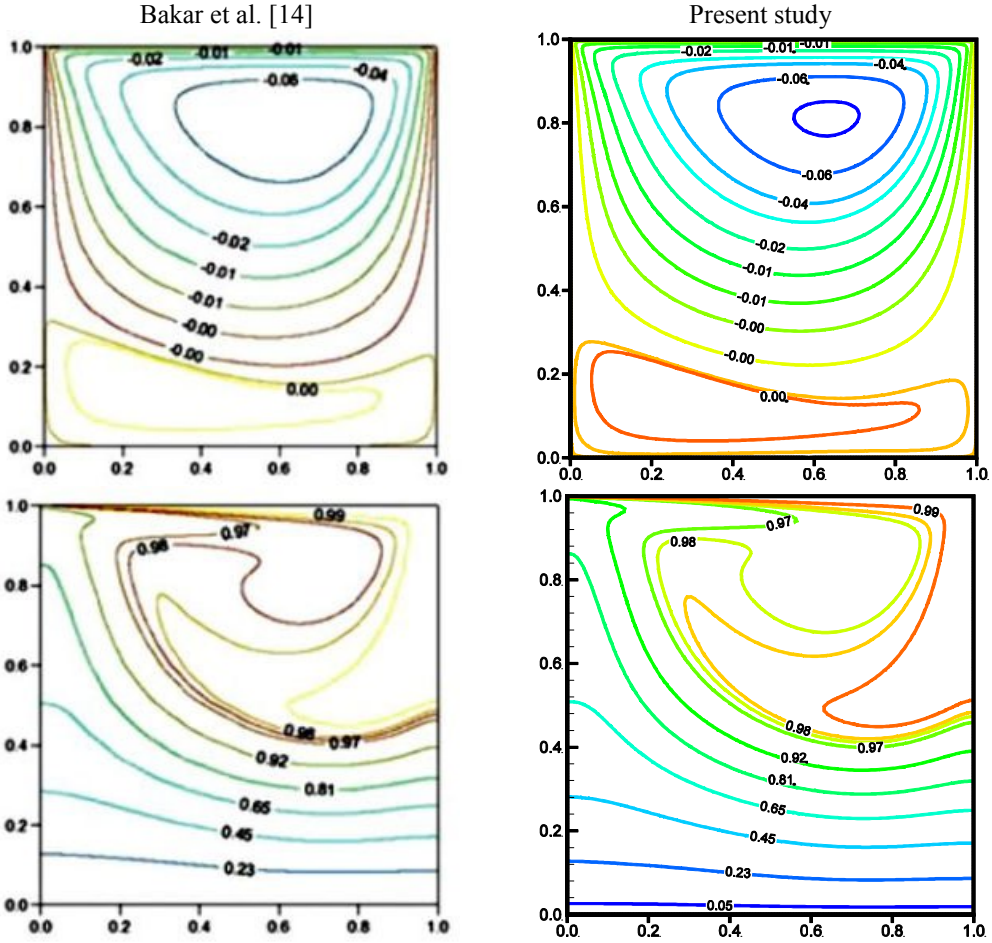

Fig.2: Comparison of streamlines (top) and isotherms (bottom) for present results with that of Bakar et al. [14].

4. Result and discussion

In this section, impacts of the pertinent parameters on flow and heat transfer through streamlines, isotherms, average Nusselt number and average temperature gives a clear explanation of fluid flow and heat transport characteristics. The diameter of the cylindrical obstacle $d = 0.2L$ considered throughout the simulation. The red color of the streamlines indicated the higher fluid velocity where the blue color corresponds to lower velocity. Similarly, the red color of isotherms also indicated the high temperature region and blue color corresponds to low temperature region.

Fig. 3 represents the impact of Reynolds number on stream field and temperature distribution for $Pr = 0.71$, $Ri = 1$, $Q = 0$, and $Ha = 10$. In Fig. 3(a), at $Re = 100$ it is seen that streamlines of the fluid flow densely moves toward the outlet where streamlines are more concentrated under the cylinder than over the cylinder. In addition, a small vortex is generated near the incoming port. After that, at $Re = 200$, the denseness is increased and a counter-clockwise rotating eddies is visible near inlet. As Re expands, counter-clockwise rotating circulation gets in large size around the obstacle. Further increase in Re, rotating cells are enlarged that occupy the most of the cavity and the strength fluid flow increases remarkably from inlet to outlet. On the other hand, in Fig. 3(b), isotherms are distributed near the left vertical as it was isothermally heated. Moreover, it occupies the half of the cavity and some isotherms are also connected with the centered cylinder as it was insulated. In addition, the isotherms are effectively close toward the hot wall as Re is increased. At each increment in Reynolds numbers, there is a clear changed in isotherms distribution compared to previous one.

Fig. 4 shows the variation of streamlines and temperature dissemination inside the cavity for different Prandtl number. In Fig. 4(a), due to inertia and buoyancy induced flow at lower *Pr*, two small cells are developed over the main flow path of both side of the obstacle. Then at $Pr = 0.71$, one of the cells is disappeared and the streamlines over the cylinder elongated towards the top left corner of the cavity. Further increasing in values of *Pr*, streamlines are more elongated toward the both top left and bottom right corners of that cavity that occupies the whole of the cavity and the small rotating cell gradually decreases for the higher *Pr*. It is important to note that higher values of Prandtl number increase fluid density which causes a reduction in fluid motion. Besides this in Fig. 4 (b) at low *Pr,* isotherm contours are distributed from right vertical wall towards the left adiabatic wall and cover the whole cavity. Then, isotherms become concentrated to the right vertical heated wall with increasing value of *Pr*. From these figures, it has been observed that thermal boundary layer are thinner near heated wall for higher value of *Pr* than that of the lower *Pr*.

Fig. 5 depicts the influence of Hartmann number on flow and temperature fields while $Q = 0$, $Re = 100$, $Pr = 0.71$ and $Ri = 1$. From Fig. 5(a), it can be seen that in the absence of magnetic field ($Ha = 0$), the recalculating cell is generated close to the stream flow over the obstruction. After that at $Ha = 10$, the recalculating cell reduced to a small vortex is created above the inlet port. From these figures it can also be seen those increased values of magnetic field, the vortex becomes smaller and finally disappeared and the flow fields occupy almost of the cavity which indicates that magnetic field effect retards the fluid motion within the cavity. In Fig. 5(b), insignificant changes are occurred in temperature distribution for increasing Hartmann number as the magnetic impact produces temperature inside the flow field.

Fig. 6 demonstrates the effect of heat generation or absorption parameter on streamline and isotherm plots while $Re = 100$, $Ri = 1$, $Pr = 0.71$ and $Ha = 10$. In Fig. 6(a), in the absence of volumetric heat generation or absorption parameter, streamlines is occupied almost of the cavity and generated a small vortex on inflow port. The flow pattern is minutely changed for the effect of volumetric heat generation or absorption upon increasing the value of heat generation or absorption

parameter. On the other hand, isotherms distribution strongly depends on the effect of heat generation or absorption parameter as shown in Fig. 6(b) which indicates that temperature fields inside the cavity are significantly affects by the heat generation or absorption. It can be observed that high temperature region is generated top side of the cavity, and also near the heated wall and finally it reaches its maximum for $Q = 10$. When heat absorption is increased, the high temperature distribution is decreased gradually and is shifted toward the right heated wall.

Figs. 7-9 demonstrate the heat transfer rate and average temperature for different combination of governing parameters. From Figs. 7(a)-9(a), it is evident that heat transfer rate monotonically increases with increasing Richardson number and which gets higher values for increased Reynolds and Prandtl number as the increased values of Prandtl number increases the fluid density which increases the energy absorbing capacity and increases Re increases fluid inertia whereas heat transfer rate decreases for increased magnetic field strength. On the other hand, average temperature profiles increase for Richardson number. It is important to note that these variations are different for the case of variation in Reynolds and Pransdtl number and also magnetic parameters as shown in Figs. 7(b)-9(b).

Fig. 10 plotted the effect of heat generation or absorption parameters on average Nusselt number and average temperature variation. In Fig. 10(a) for all $Q < 0$, it can be easily seen that heat transfer rate gradually increases whereas heat transfer rate gradually decreases for all $Q > 0$. The reason behind it is that higher heat generation parametric values increase fluid temperature whereas absorption parameters reduce fluid temperature. Consistent behavior is also found in average temperature shown in Fig. 10(b). These variation for $Q > 0$ in both Figs. 10 (a) and 10 (b) are depend Richardson number.

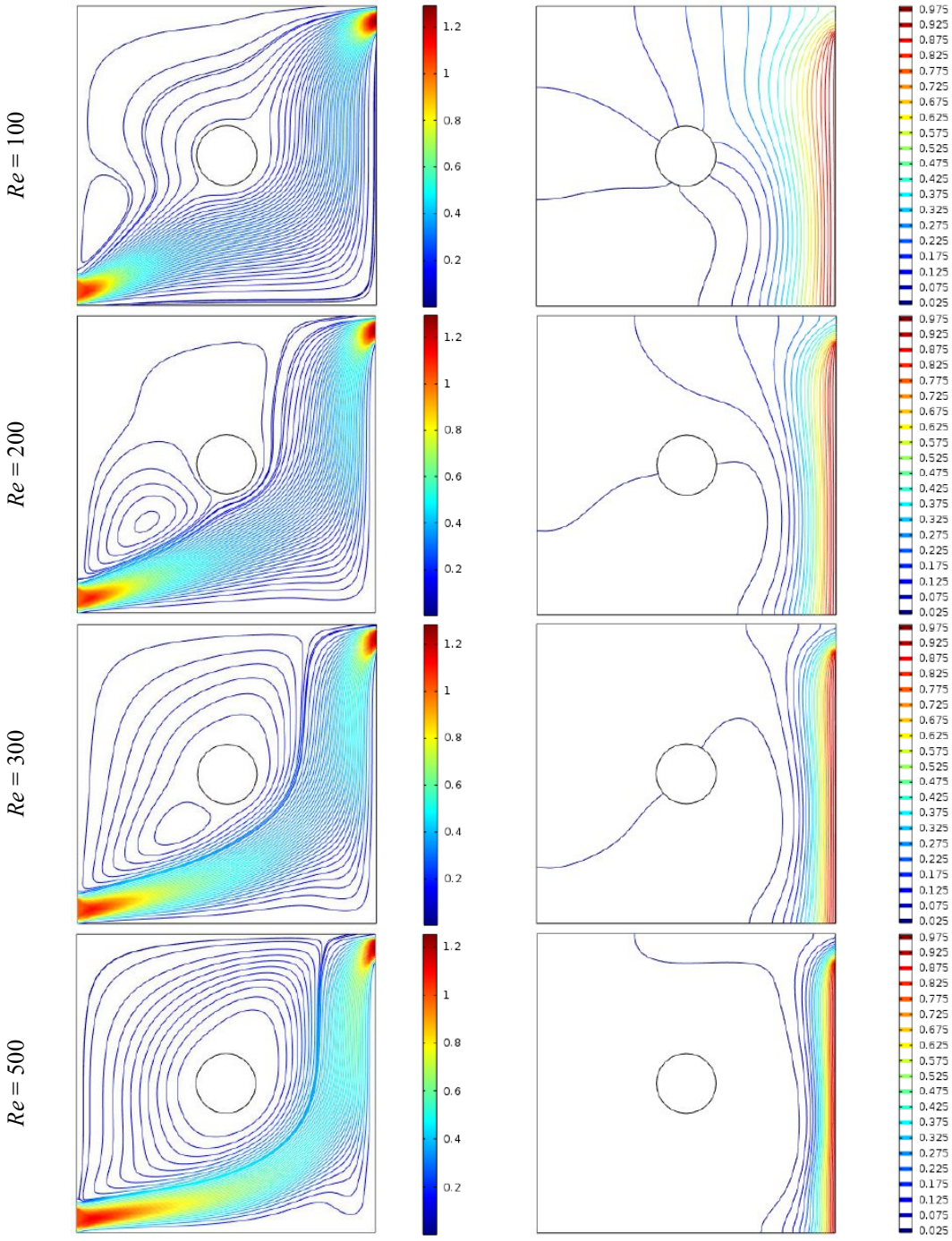

Fig. 3: (a) Streamlines (b) Isotherms for various *Re* while *Pr* = 0.71, *Ri* = 1, *Q* = 0, and *Ha* = 10.

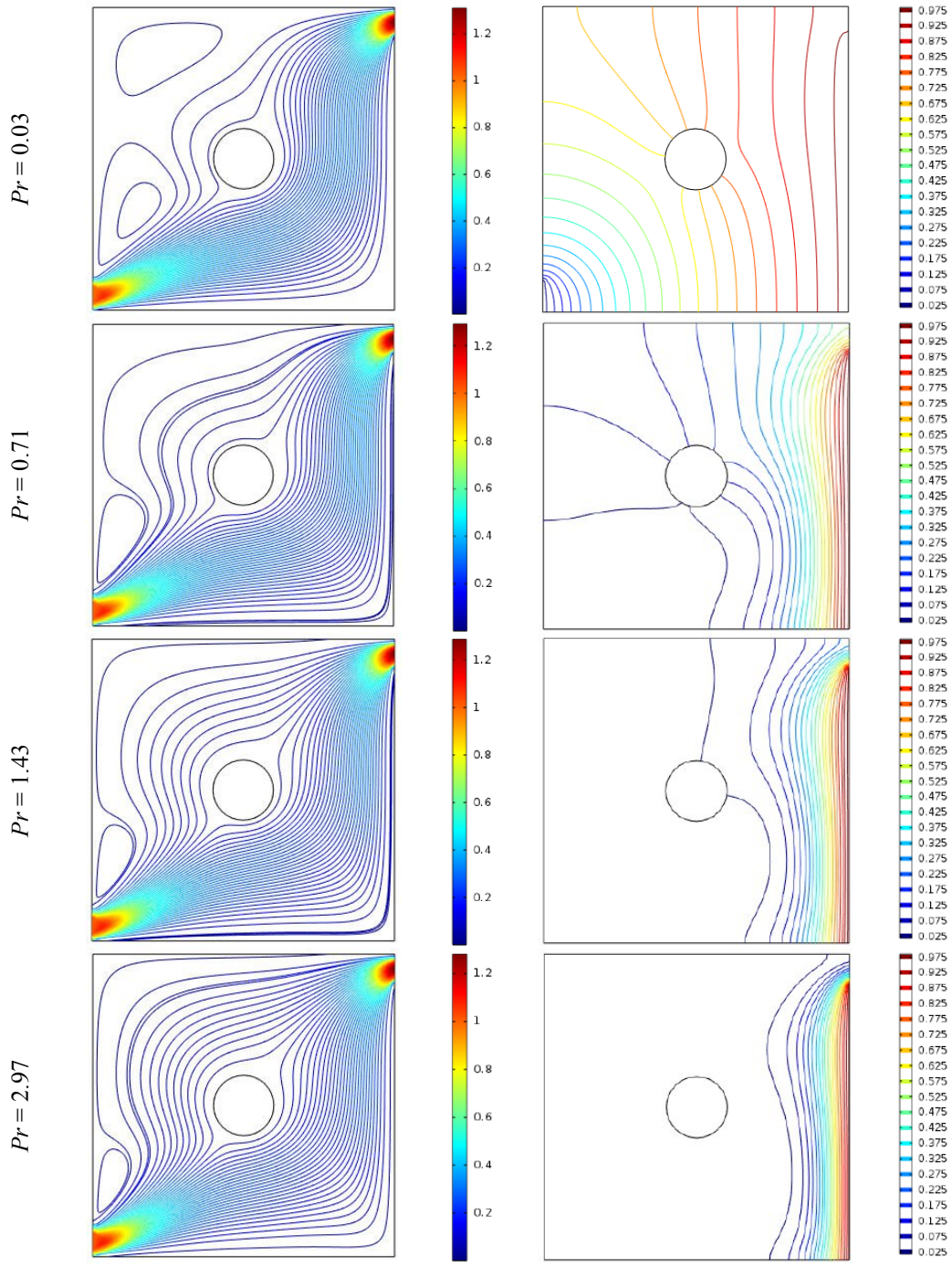

Fig. 4: (a) Streamlines and (b) Isotherms for various *Pr* while *Re* = 100, *Ri* = 1, *Q* = 0, and *Ha* = 10.

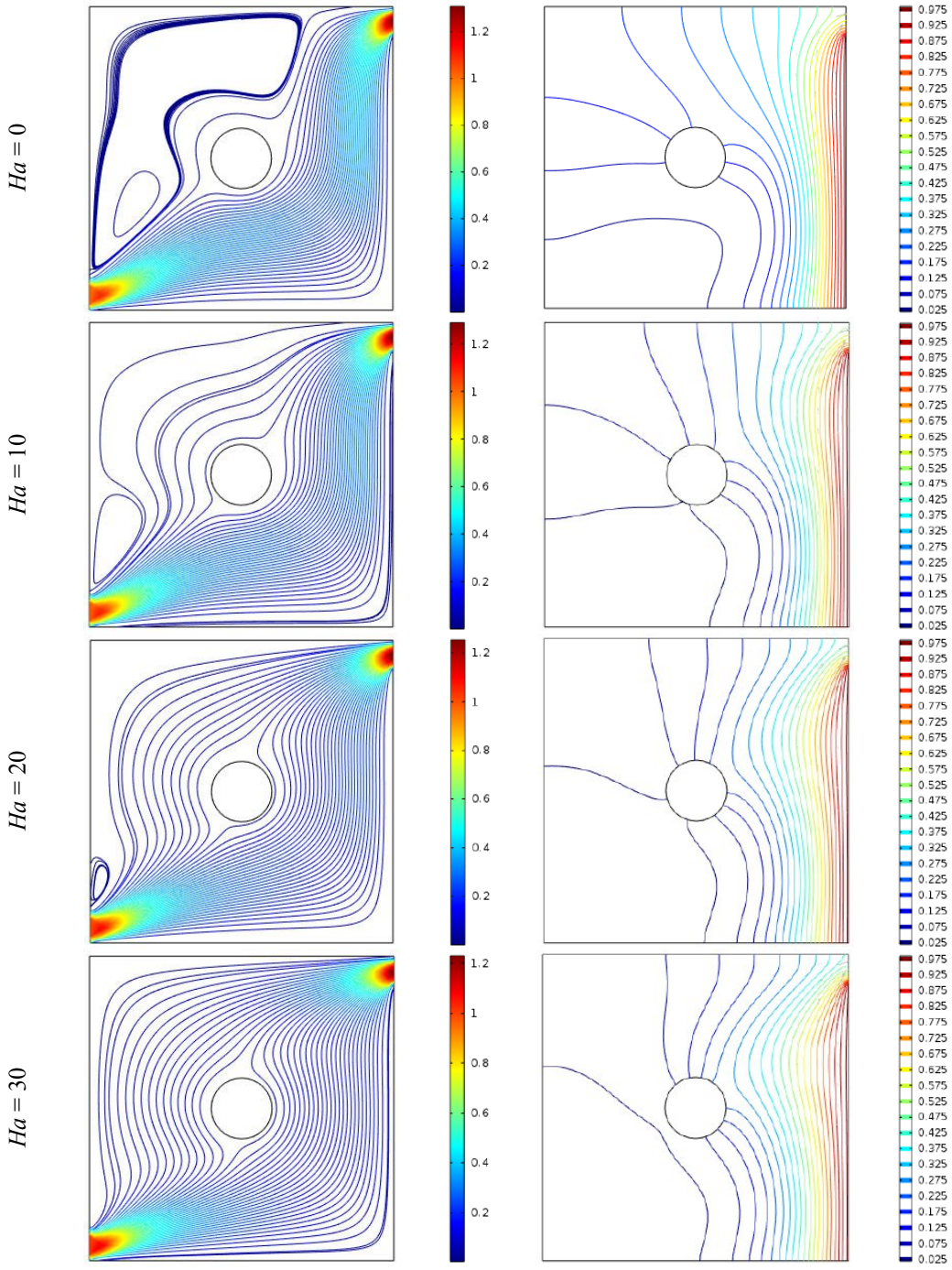

(a) (b)

Fig. 5: (a) Streamlines (b) Isotherms for various *Ha* while *Re* = 100, *Ri* = 1, *Q* = 0, and *Pr* = 0.71.

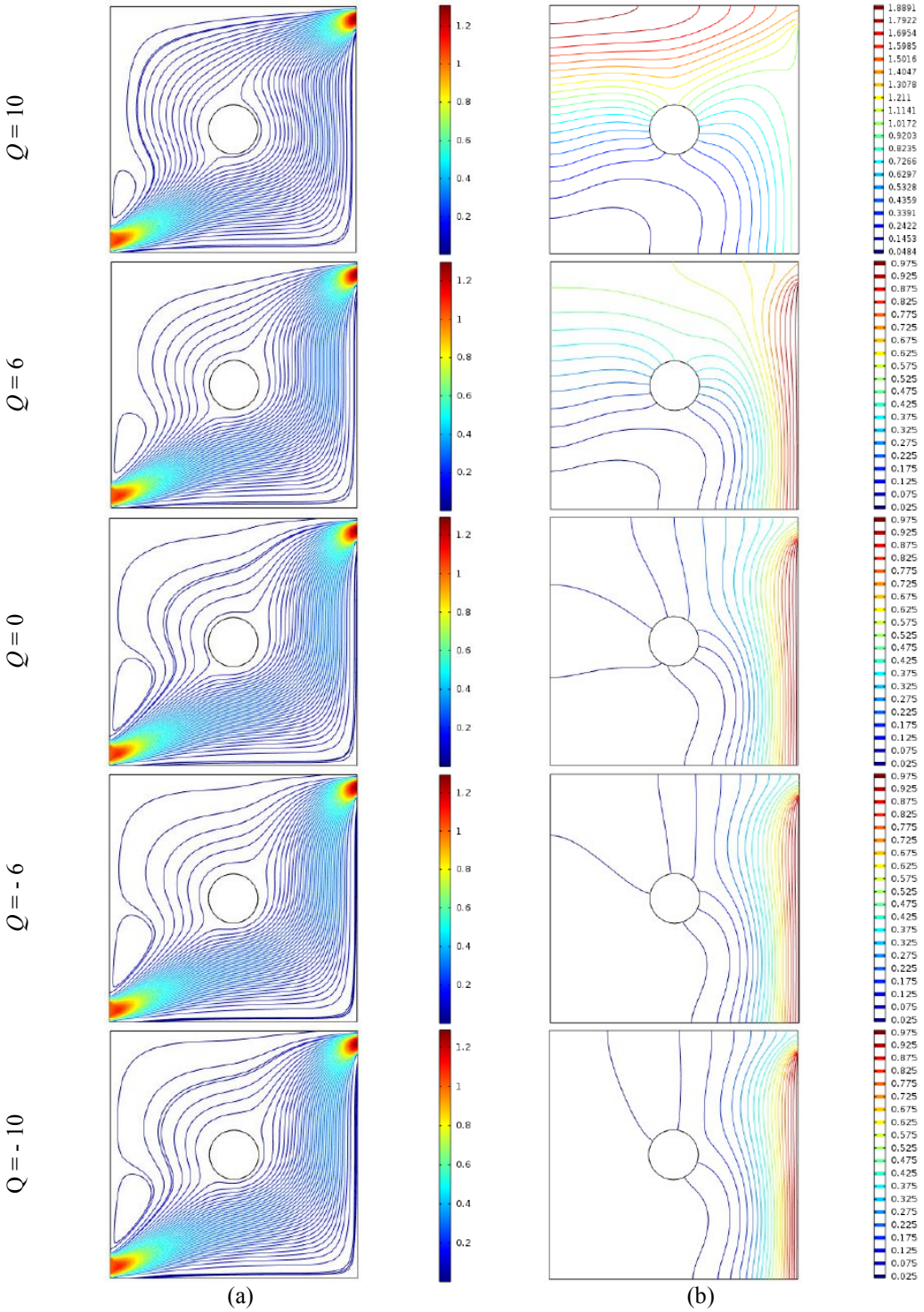

Fig. 6: (a) Streamlines (b) Isotherms for various Q while $Ha = 10$, $Pr = 0.71$, $Ri = 1$, and $Re = 100$.

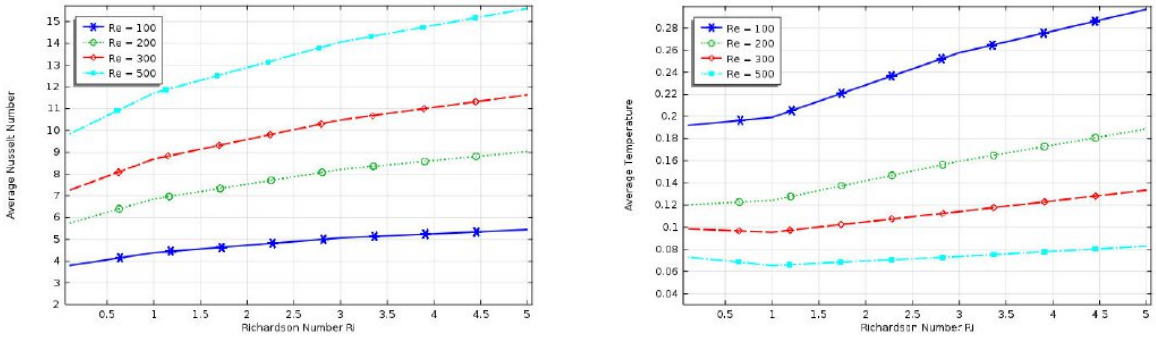

(a) (b)

Fig. 7: Variation of (a) Average Nusselt number, (b) Average temperature for *Re* while *Pr* = 0.71, *Q* = 0 and *Ha* = 10.

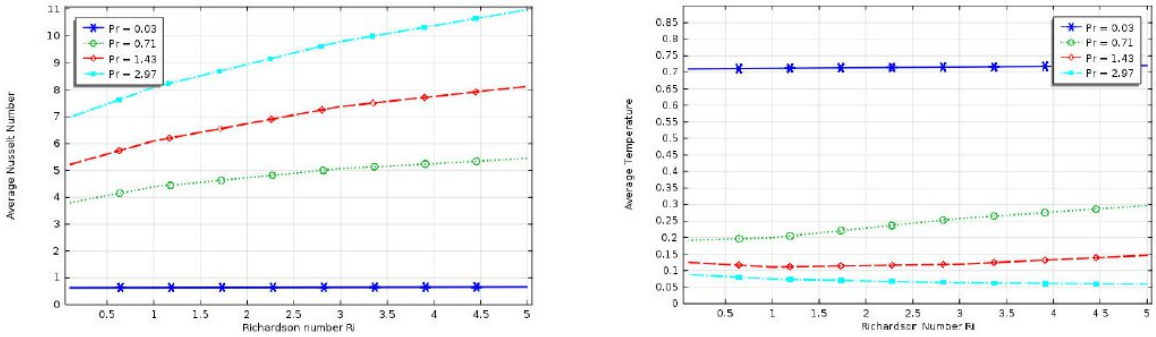

(a) (b)

Fig. 8: Variation of (a) Average Nusselt number, (b) Average temperature for *Pr* while *Q* = 0, *Re* = 100 and *Ha* = 10.

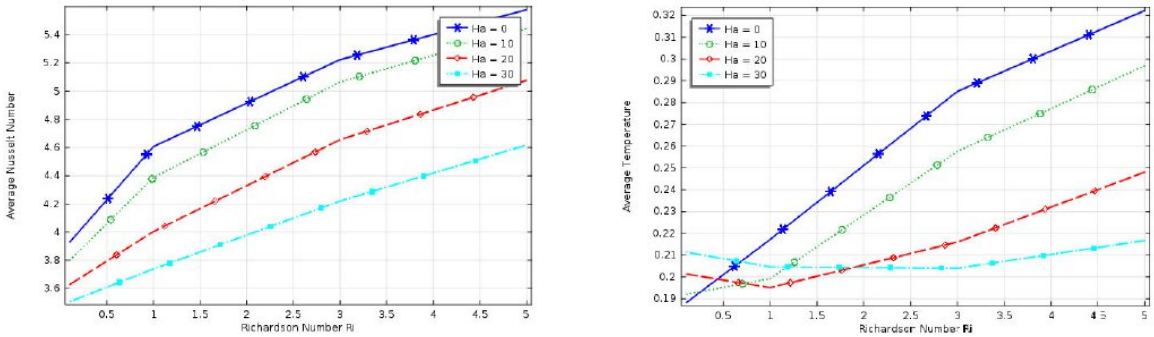

(a) (b)

Fig. 9: Variation of (a) Average Nusselt number, (b) Average temperature for *Ha* while *Q* = 0, *Re* = 100 and *Pr* = 0.71.

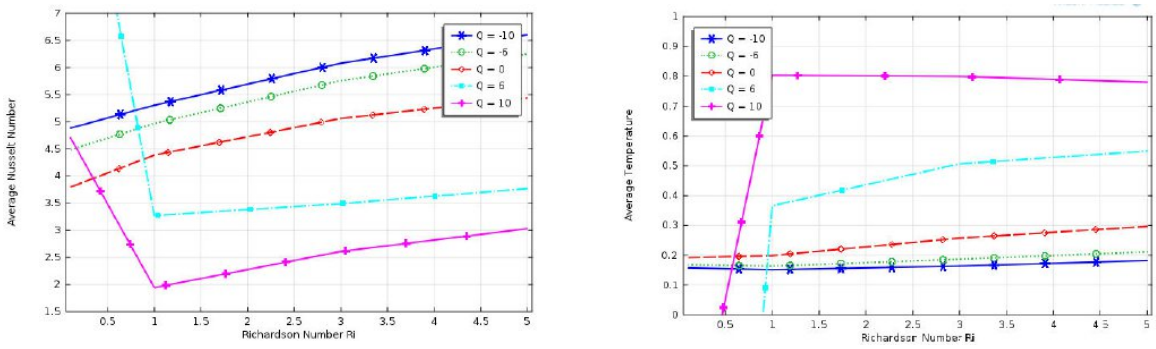

(a) (b)

Fig. 10: Variation of (a) Average Nusselt number, (b) Average temperature for Q while Ha = 10, Re = 100 and Pr = 0.71.

5. Conclusion

The above study has been numerically investigated and the conclusions are to find out and listed as follows:

- The flow and temperature distributions have remarkable changed for Reynolds number. The heat transfer rate enhancing with increasing Re. Also, it is obtained that maximum Nu_{av} and minimum θ_{av} for highest Re.
- Thermal layers near the right vertical wall become thinner with increasing Pr. Moreover, Nu_{av} increases and θ_{av} inversely decreases with increasing Pr.
- Due to the strength of magnetic field, flow and heat transfer characteristics have noticeably changed. The highest Nu_{av} is acquired inside the cavity in absence of magnetic field.
- Streamlines and isotherms have practically invariant due to heat generation or absorption parameter. Also, minimum θ_{av} is found in presence of heat absorption.

Acknowledgements

The author would like to acknowledge the financial support received from the National Science and Technology (NST) fellowship 2018-19 in physical science (Grant ID-6322, BDT-54,000 (USD-637.43)), Bangladesh.

References

[1] T. Basak, S. Roy, P. K. Sharma, I. Pop, Analysis of mixed convection flows within a square cavity with linearly heated side wall (s), International Journal of Heat and Mass Transfer, 52(9-10) (2009) 2224-2242.

[2] T Basak, S. Roy, S. K. Sing, I. Pop, "Analysis of mixed convection in a lid driven porous square cavity with linearly heated side walls", International Journal of Heat and Mass transfer, 53 (2010) 1819-1840.

[3] M. A. Hassan, S. Jamal, Mixed convection in lid driven square cavity using finite volume method, In Applied Mechanics and Materials, 592 ((2014) 1652-1656.

[4] A. Charttopadhyay, S. K, Pandit, S. S. Sarma, I. Pop, Mixed convection in a double lid-driven sinusoidally heated porous cavity, International Journal of Heat and Mass Transfer, 93 (2016) 361-378.

[5] S. Mekroussi, S. Kherris, B. Mebarki, A. Benchatti, Mixed convection in complicated cavity with non-uniform heating on both sidewalls, Int J Heat Technol, 35(4) (2017) 1023-1033.

[6] F. M. Azizul, A. I. Alsabery, I. Hashim, A.J. Chamkha, Heatline visualization of mixed convection inside double lid-driven cavity having heated wavy wall, Journal of Thermal Analysis and Calorimetry, (2020) 1-18.

[7] M. J. Uddin, A. F. Hoque, M. M. Rahman, K. Vajravelu, Numerical simulation of convective heat transport within the nanofluid filled vertical tube of plain and uneven side walls, International Journal of Thermofluid Science and Technology, 6(1) (2019) 19060101.

[8] M. Fayz-Al-Asad, M. J. H. Munshi, M. M. A. Sarker, Effect of Fin Length and Location on Natural Convection Heat Transfer in a Wavy

Cavity, International Journal of Thermofluid Science and Technology, 7(3) (2020) 070303.

[9] T. Islam, N. Parveen, M. F. Asad, Hydromagnetic natural convection heat transfer of copper-water nanofluid within a right-angled triangular cavity, International Journal of Thermofluid Science and Technology, 7(3) (2020) 070304.

[10] M. M. Rahman, M. Elias, M. A. Alim, Mixed convection flow in a rectangular ventilated cavity with a heat conducting solid circular cylinder at the center, Journal of Engineering and Applied Sciences, 24(1) (2009) 20-29.

[11] M .M. Rahman, M.A. Alim, MHD mixed convection flow in a vertical lid-driven square enclosure including a heat conducting horizontal circular cylinder with joule heating, Nonlinear analysis: Modeling and Control, 17 (2010) 199-211.

[12] Mohammad Mokaddes Ali, M. A. Alim, S. S. Ahmed, Magnetohydrodynamic Mixed Convection Flow in a Hexagonal Enclosure, Procedia Engineering 194 (2017) 479 – 486.

[13] F. S. Oğlakkaya, C. Bozkaya, Unsteady MHD mixed convection flow in a lid-driven cavity with a heated wavy wall, International Journal of Mechanical Sciences, 148 (2018) 231-245.

[14] N. A. Bakar, R. A. Roslan, R., Karimipour, I. Hashim, Mixed convection in lid-driven cavity with inclined magnetic field, Sains Malaysiana, 48(2) (2019) 451-471.

[15] A. Sarkar, M. A., Alim, M. J. H. Munshi, M. M. Ali, Numerical study on MHD mixed convection in a lid driven cavity with a wavy top wall and rectangular heaters at the bottom. In AIP conference proceedings, 2121 (2019) 030004.

[16] B. P. Geridonmez, H. F. Oztop, Mixed convection heat transfer in a lid-driven cavity under the effect of a partial magnetic field, Heat Transfer Engineering, 42(10) (2021) 875-887.

[17] A.J. Chamkha, Hydromagnetic combined convection flow in a vertical lid-driven cavity with internal heat generation or absorption, Numerical Heat Transfer, Part A 41 (2002) 529-546.

[18] L. K. Saha, K. M. S. Uddin, M. A. Taher, Effect of internal heat generation or absorption on MHD mixed convection flow in a lid driven cavity, American Journal of Applied Mathematics 3(3) (2015) 20–29.

[19] S. Hussain, H. F. Oztop, Khalid Mehmood, Nidal Abu-Hamdeh," Effects of inclined magnetic field on mixed convection in ananofluid filled double lid-driven cavity with volumetric heat generation or absorption using finite element method", Chinese Journal of Physics(2018).

[20] C. Taylor, P. Hood, A numerical solution of the Navier-Stokes equations using finite element technique, Computer and Fluids, 1 (1973) 73-89.

[21] P. Dechaumphai, Finite Element Method in Engineering, 2nd ed. Chulalongkorn University Press, Bangkok, (1999).

[22] R. Akhter, M. M. Ali, M. A. Alim, Hydromagnetic natural convection heat transfer in a partially heated enclosure filled with porous medium saturated by nanofluid, International Journal of Applied and Computational Mathematics, 5(3) (2019) 1-27.

[23] M. M. Ali, R. Akhter, M. A. Alim, MHD natural convection and entropy generation in a grooved enclosure filled with nanofluid using two-component non-homogeneous model, SN Applied Sciences, 2(4) (2020) 1-25.